Available online at www.sciencedirect.com

SciVerse ScienceDirect

Ceramics International 38 (2012) 6903–6906

CERAMICS INTERNATIONAL

www.elsevier.com/locate/ceramint

Short communication

Optimization of energy storage density in ANb$_2$O$_6$–NaNbO$_3$–SiO$_2$ (A=[(1−x)Pb, xSr]) nanostructured glass–ceramic dielectrics

D.F. Han, Q.M. Zhang, J. Luo, Q. Tang, J. Du*

Advanced Electronic Materials Institute, General Research Institute for Nonferrous Metals, Beijing 100088, PR China

Received 21 March 2012; received in revised form 28 April 2012; accepted 28 April 2012
Available online 9 May 2012

Abstract

The substitution effect of Sr for Pb at A-site was studied for the purpose of energy storage density optimization in ANb$_2$O$_6$–NaNbO$_3$–SiO$_2$ (A=[(1−x)Pb, xSr]) glass–ceramic dielectrics. At the point of x=0.6, nanostructured glass–ceramics with the highest dielectric constant (~600) and a relatively high breakdown strength (36.7 kV/mm) were acquired, resulting in the highest energy storage density of 2.27 J/cm^3, which is twice higher than those of the end-products (i.e., x=0 and x=1.0).

Keywords: C. Dielectric properties; D. Niobates; D. Glass–ceramics; Energy storage density

1. Introduction

Glass–ceramic dielectrics have long been considered as the most promising candidate for energy storage capacitors [1–3], with the synergistic effect of high permittivity (from the precipitated ceramic phases) [4] and high breakdown strength (due to the pore-free inherence) [5]. Titanates and niobates based glass–ceramic dielectrics are the most studied materials. As an important titanates based system, (Ba, Sr)TiO$_3$ based glass–ceramics can exhibit high dielectric constant and high breakdown strength though the addition of the other oxide and fluoride components [6,7] and the adjustment of Ba/Sr [3] and Ba/Ti [8] ratios. However, the acquired values of their energy storage density calculated by polarization hysteresis measurements are low [3,9]. Gorzkowski et al. found high dielectric constant of ~1000 and high breakdown strength of 80 kV/mm, but low energy density of 0.3–0.9 J/cm^3 in (Ba, Sr)TiO$_3$ based glass–ceramics [3]. For another attractive system, niobates based glass–ceramics, such as PbO–Na$_2$O–Nb$_2$O$_5$–SiO$_2$ [4,5], BaO–Na$_2$O–Nb$_2$O$_5$–SiO$_2$ [10,11], SrO–K$_2$O–Nb$_2$O$_5$–SiO$_2$ [11] and PbO–BaO–SrO–Nb$_2$O$_5$–B$_2$O$_3$–SiO$_2$ [12] glass–ceramics, have also been investigated widely. Some of these glass–ceramics are believed to have a great potential to achieve high energy density for promising applications.

Element substitution is a common and effective method to improve the microstructure and dielectric properties of dielectric ceramics [13,14]. The improvement of the dielectric properties through element substitution can result in the optimization of the energy storage density of the dielectric ceramics. Fletcher et al. studied the energy-storage behavior of the sintered (Ba, Sr)TiO$_3$ ceramics and found the adjustment of the substitution fraction of Sr for Ba could optimize the energy density in the dielectrics and that the highest energy density was usually achieved when about 80% Ba was substituted by Sr [15]. Most these kind of substitution work are focused on improving dielectric properties of sintered ceramics. However, few details have been reported on the effect of the element substitution on the energy-storage behavior of glass–ceramic dielectrics. It is believed that the similar work upon glass–ceramics would bring them considerable improvements on energy storage density.

In this paper, the element substitution effect of Sr for Pb was systematically studied for the purpose of energy storage density optimization in ANb$_2$O$_6$–NaNbO$_3$ –SiO$_2$ (A=[(1−x)-Pb, xSr]) nanostructured glass–ceramics dielectrics. The dielectric constant and the breakdown strength were used to

*Corresponding author. Tel.: +86 10 82241247; fax: +86 10 82241246.
E-mail address: dujun@grinm.com (J. Du).

0272-8842/$36.00 © 2012 Published by Elsevier Ltd and Techna Group S.r.l.
http://dx.doi.org/10.1016/j.ceramint.2012.04.087

describe qualitatively the energy density behavior. The above dielectric performance was analyzed and discussed from the point of view on the phase development and microstructural evolution for different substitution fractions x of the final nanostructured glass–ceramics.

2. Experimental procedures

The nominal composition of $10[(1-x)PbO-xSrO]$–$20Na_2O$–$40Nb_2O_5$–$30SiO_2$ ($x=0$–1.0) was used in this study, which was predicted to form $(50ANb_2O_6+50NaNbO_3)_{ceramic}+(SiO_2)_{glass}$ ($A=[(1-x)Pb, xSr]$) glass–ceramics. Analytical reagent grade powders of $SrCO_3$ ($\geq 99.5\%$), Na_2CO_3 ($\geq 99.5\%$), PbO ($\geq 99.5\%$), Nb_2O_5 ($\geq 99.5\%$) and SiO_2 ($\geq 99.5\%$) were well mixed and then melted at 1400 °C for 3 h in platinum crucible to form molten glass followed by quick-casting into a preheated stainless steel mold to form glass bulks. The controlled crystallization was carried out at 850 °Cfor 3 h to result in the final nanostructured glass–ceramic dielectrics.

X-ray diffraction was performed on high-resolution X'Pert PRO diffractometer using CuK_α radiation. Microstructural observation was carried out using a transmission electron microscope (TEM: JEOL 2010F, 200 kV). The dielectric measurements were carried out on glass–ceramic sheets of 0.20–0.25 mm in thickness with Au electrodes sputtered on both surfaces. The polarization was measured at room temperature using a ferroelectric tester (RT6000HVA, Radiant Technology, Albuquerque, NM). The dielectric constant was carried out using an Agilent 4284 A precision LCR meter (Santa Clara, CA). The DC breakdown strength was measured using a combination of Tektronix AFG 3021 Arbitrary/Function Generator (Beaverton, OR) and Trek Model 30/20 A high-voltage amplifier (Beaverton, OR). All samples were immersed in silicon oil to prevent surface flashover.

3. Result and discussion

The P–E curves measured under a unipolar E up to breakdown for all the samples are shown in Fig. 1(a). It is seen that the glass–ceramics, especially for the samples with the substitution fractions of $x \geq 0.4$ exhibit almost a linear P–E relationship even at high electric field, indicating excellent electric field stability of dielectric constant. This is mainly due to weak ferroelectric properties of dielectric particles in nanometer size [16] and paraelectric glass phase. Energy density (Fig. 1(b)) was estimated from the P–E curves, by integrating the area enclosed within the polarization axis and the discharged curve. The energy densities for both the end-products at $x=0$ and $x=1.0$ are 0.872 J/cm^3 and 0.988 J/cm^3, respectively. The highest energy density of 2.27 J/cm^3 is found at $x=0.6$, which is more than twice as high as those of the end-products. Qualitatively, it is known that the energy density of a linear dielectric material in electric field E is given by $U_{BD}=1/2\varepsilon_0\varepsilon_r E_{BD}^2$ [5], indicating the stored energy density (U_{BD}) is proportional to the dielectric constant (ε_r) and the square of breakdown strength (E_{BD}).

Fig. 2 shows the substitution fraction x dependence of dielectric constant (measured at 1 kHz) and breakdown strength of the glass–ceramics. The dielectric constant exhibits a parabolic relationship with the substitution fraction x varying from 0 to 1.0 and the maximum dielectric constant of ~600 is located near $x=0.6$. For sintered $Pb_{1-y}Ba_yNb_2O_6$ ceramics [14], a similar relationship between the dielectric constant and Pb/Ba ratio was also observed due to the existence of MPB region near $y=0.63$. In general, the dielectric performance could be largely enhanced at a composition near the MPB region. Thus, the maximum dielectric constant for $x=0.6$ is obviously related to the MPB phenomenon in the crystallized tungsten–bronze particles. The powder x-ray diffraction (XRD) data for the glass–ceramics are shown in Fig. 3. As can be seen, besides the perovskite $NaNbO_3$

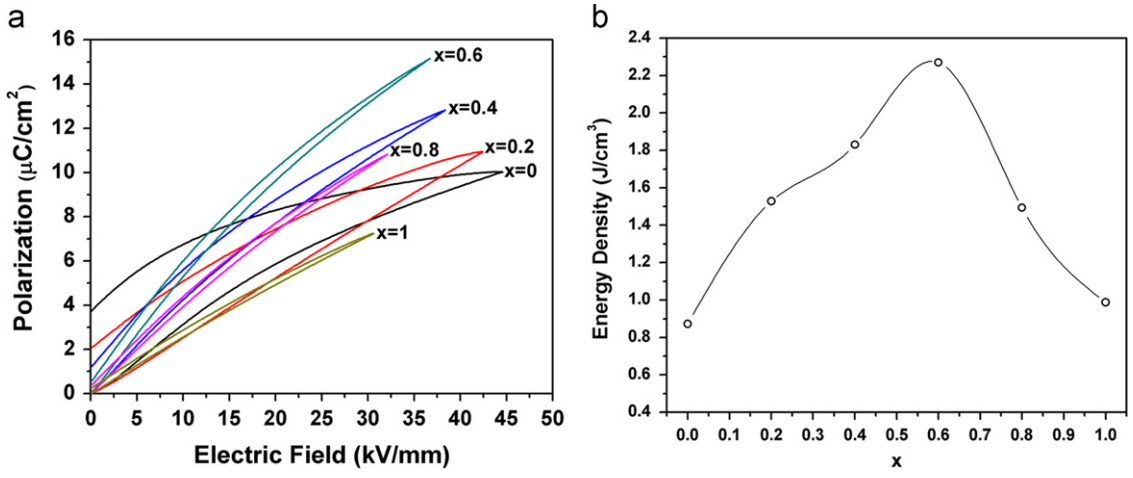

Fig. 1. (a) P–E curves measured under a unipolar E of 10 Hz up to breakdown for samples crystallized at 850 °C for 3 h. (b) Energy storage density as a function of substitution fraction x of the glass–ceramics.

phase found to exist in all composites, tungsten–bronze $A\mathrm{Nb_2O_6}$ ($A=[(1-x)\mathrm{Pb}, x\mathrm{Sr}]$) is another principal dielectric phase. When the substitution fraction x is less than 0.6, the tungsten–bronze phase can be indexed in the orthorhombic structure, while for the case of substitution fraction over 0.6, the tungsten–bronze phase belongs to the tetragonal structure. It further indicates that an MPB between the orthorhombic and tetragonal tungsten–bronze phases exists near $x=0.6$, although the glass–ceramics are prepared through melt-quenching followed by controlled crystallization.

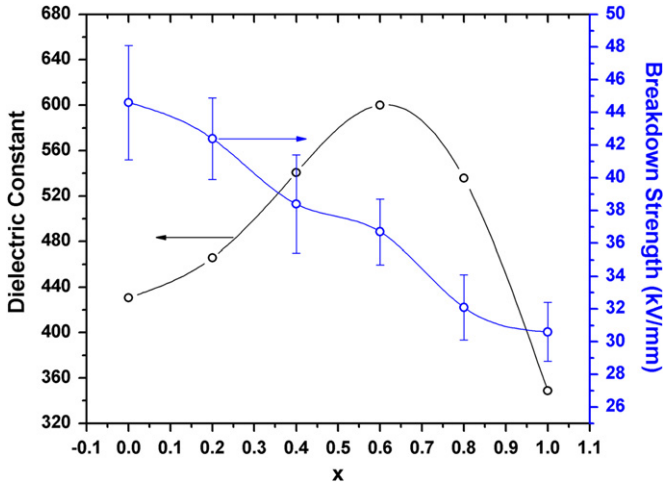

Fig. 2. Dielectric constant and breakdown strength as a function of substitution fraction x of the glass–ceramics.

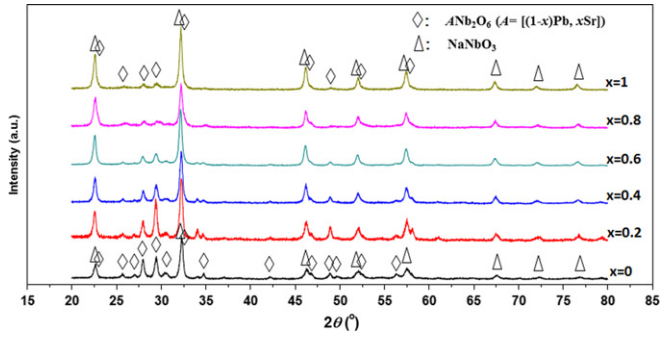

Fig. 3. Powder x-ray diffraction patterns for the glass–ceramic samples.

The breakdown strength of the glass–ceramics (shown in Fig. 2) decreases from 44.6 kV/mm to 31.0 kV/mm when the substitution fraction x is varied from 0 to 1.0. At $x=0.6$ corresponding to the composition of MPB region, the breakdown strength of the glass–ceramic is 36.7 kV/mm. The variation of dielectric strength was discussed from the point of view on the microstructural evolution of the glass–ceramics with different substitution fractions x.

The TEM micrographs of the as-prepared glass–ceramics are shown in Fig. 4. The crystalline particles obviously exhibit various shapes in the glass–ceramics with different substitution fractions x. Microstructure of the sample with $x=0$ (Fig. 4(a)) shows the shape of crystallized ceramic particles is spherical and the size is in several tens of nm. Comparatively, typical dendritic microstructures are observed in the glass–ceramics with the substitution fraction of $x=0.6$, while the sample with $x=1$ exhibits larger dendritic particles in length than the sample with $x=0.6$. It is suggested that, as substitution fraction x increases, the reduction of dielectric strength is primarily due to the gradual variation of grain shape from sphere to dendrite in the glass–ceramic dielectrics. The effect of dendrites on breakdown strength in glass–ceramic dielectrics has also been reported previously [3,8]. The results show that it is deleterious to the breakdown strength due to a high field concentration at the tips of the dendrites, causing premature failure.

As discussed above, when the substitution fraction x is varied from 0 to 1.0, the variation of dielectric constant and breakdown strength collectively optimized the energy density. For the substitution fraction of $x=0.6$ near the MPB region between $\mathrm{PbNb_2O_6}$ and $\mathrm{SrNb_2O_6}$, the maximum dielectric constant and moderate breakdown strength contribute to the highest energy density.

4. Conclusions

The substitution effect of Sr for Pb at A-site in nanostructured $A\mathrm{Nb_2O_6}$–$\mathrm{NaNbO_3}$–$\mathrm{SiO_2}$ ($A=[(1-x)\mathrm{Pb}, x\mathrm{Sr}]$) glass–ceramic dielectrics is systematically studied for the purpose of energy storage density optimization.

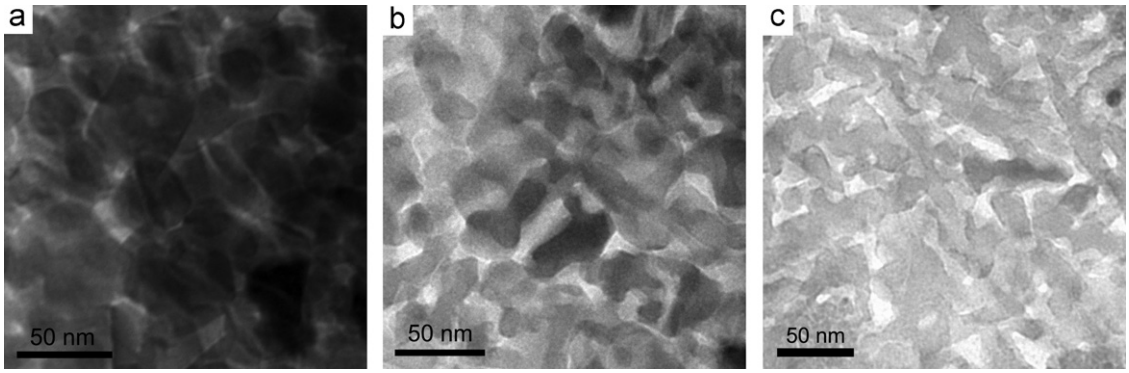

Fig. 4. Bright-field TEM micrographs for the glass–ceramics with (a) $x=0$, (b) $x=0.6$ and (c) $x=1$.

The energy densities for both the end-products at $x=0$ and $x=1.0$ are 0.872 J/cm^3 and 0.988 J/cm^3, respectively, while the highest energy density of 2.27 J/cm^3 is found at $x=0.6$, which is more than twice as high as those of the end-products. The breakdown strength decreases from 44.6 kV/mm to 31.0 kV/mm when the substitution fraction x is varied from 0 to 1.0. The microstructure analysis indicates that the reduction of breakdown strength is attributed to the gradual variation of particle shape from sphere to dendrite. The dielectric constant shows a parabolic relationship with the substitution fraction, and the maximum dielectric constant of $\sim$600 is located at $x=0.6$. Perovskite $NaNbO_3$, tungsten–bronze ANb_2O_6 ($A=[(1-x)Pb, xSr]$) phases and glass phase coexist in the glass–ceramic dielectrics, and an MPB between $PbNb_2O_6$ and $SrNb_2O_6$ phases is formed near $x=0.6$, resulting in the maximum dielectric constant, which was believed to be the main contribution to the optimized energy density.

Acknowledgment

The authors acknowledge the financial support from the National High-tech Program (863 program) under grant No. 2008AA03A236 and the Project 51107005 supported by National Natural Science Foundation of China.

References

[1] A. Herezog, Applications of glass–ceramics for electronic components and circuits, IEEE Transactions on Parts, Hybrids, and Packaging PHP 9 (1973) 247–256.
[2] G.H. Beall, Synthesis and design of glass–ceramics, Journal of Material Education 14 (1992) 315–361.
[3] E.P. Gorzkowski, M.-J. Pan, B. Bender, C.C.M. Wu, Glass–ceramics of barium strontium titanate for high energy density capacitors, Journal of Electroceramics 18 (2007) 269–276.
[4] J. Du, B. Jones, M. Lanagan, Preparation and characterization of dielectric glass–ceramics in Na_2O–PbO–Nb_2O_5–SiO_2 system, Materials Letters 59 (2005) 2821–2826.
[5] J. Luo, J. Du, Q. Tang, C.H. Mao, Lead sodium niobate glass–ceramic dielectrics and internal electrode structure for high energy storage density capacitors, IEEE Transactions on Electron Devices 55 (2008) 3549–3554.
[6] E.P. Gorzkowski, M.-J. Pan, B.A. Bender, C.C.M. Wu, Effect of additives on the crystallization kinetics of barium strontium titanate glass–ceramics, Jorunal of the American Ceramic Society 91 (2008) 1065–1070.
[7] J.C. Chen, Y. Zhang, C.S. Deng, X.M. Dai, Improvement in the microstructures and dielectric properties of barium strontium titanate glass–ceramics by AlF_3/MnO_2 addition, Journal of the American Ceramic Society 92 (2009) 1863–1866.
[8] J.C. Chen, Y. Zhang, C.S. Deng, X.M. Dai, L.T. Li, Effect of the Ba/Ti ratio on the microstructures and dielectric properties of barium titanate-based glass–ceramics, Journal of the American Ceramic Society 92 (2009) 1350–1353.
[9] Y. Zhang, J.J. Huang, T. Ma, X.R. Wang, C.S. Deng, X.M. Dai, Sintering temperature dependence of energy-storage properties in (Ba, Sr)TiO_3 glass–ceramics, Journal of the American Ceramic Society 94 (2011) 1805–1810.
[10] B. Rangarajan, B. Jones, T. Shrout, M. Lanagan, Barium/lead-rich high permittivity glass–ceramics for capacitor applications, Journal of the American Ceramic Society 90 (2007) 784–788.
[11] F. Peng, R.F. Speyer, W. Hackenberger, Devitrification and dielectric properties of (Na_2O, BaO)–Nb_2O_5–SiO_2 and (K_2O, SrO)–Nb_2O_5–SiO_2 glass–ceramics, Journal of Material Research 22 (2007) 1996–2003.
[12] C.-T. Cheng, M. Lanagan, B. Jones, J.-T. Lin, M.-J. Pan, Crystallization kinetics and phase development of PbO–BaO–SrO–Nb_2O_5–B_2O_3–SiO_2-based glass–ceramics, Journal of the American Ceramic Society 88 (2005) 3037–3042.
[13] J.R. Oliver, R.R. Neurgaonkar, L.E. Cross, Ferroelectric properties of tungsten bronze morphotropic phase boundary systems, Journal of the American Ceramic Society 72 (1989) 202–211.
[14] R. Guo, A.S. Bhalla, C.A. Randall, Z.P. Chang, L.E. Cross, Polarization mechanisms of morphotropic phase boundary lead barium niobate (PBN) compositions, Journal of Applied Physics 67 (1990) 1453–1460.
[15] N.H. Fletcher, A.D. Hilton, B.W. Ricketts, Optimization of energy storage density in ceramic capacitors, Journal of Physics D: Applied Physics 29 (1996) 253–258.
[16] K. Kyoichi, Y. Akihiko, Grain-size effects on dielectric properties in barium titanate ceramics, Journal of Applied Physics 47 (1976) 371–373.